APL Materials

$LaTiO_3/KTaO_3$ interfaces: A new two-dimensional electron gas system

Cite as: APL Mater. **3**, 036104 (2015); https://doi.org/10.1063/1.4914310
Submitted: 19 December 2014 • Accepted: 23 February 2015 • Published Online: 05 March 2015

K. Zou, Sohrab Ismail-Beigi, Kim Kisslinger, et al.

ARTICLES YOU MAY BE INTERESTED IN

Research Update: Conductivity and beyond at the $LaAlO_3/SrTiO_3$ interface
APL Materials **4**, 060701 (2016); https://doi.org/10.1063/1.4953822

Two-dimensional electron systems and interfacial coupling in $LaCrO_3/KTaO_3$ heterostructures
Applied Physics Letters **118**, 192905 (2021); https://doi.org/10.1063/5.0049119

Evolution of ferromagnetism in two-dimensional electron gas of $LaTiO_3/SrTiO_3$
Applied Physics Letters **112**, 122405 (2018); https://doi.org/10.1063/1.5009768

AMERICAN ELEMENTS
THE ADVANCED MATERIALS MANUFACTURER
The Next Generation of Material Science Catalogs
Now Invent.
www.americanelements.com

© 2015 Author(s).

APL MATERIALS 3, 036104 (2015)

$LaTiO_3/KTaO_3$ interfaces: A new two-dimensional electron gas system

K. Zou,[1] Sohrab Ismail-Beigi,[1] Kim Kisslinger,[2] Xuan Shen,[2,3] Dong Su,[2] F. J. Walker,[1] and C. H. Ahn[1]
[1]*Department of Applied Physics and Center for Research on Interface Structures and Phenomena (CRISP), Yale University, New Haven, Connecticut 06520, USA*
[2]*Brookhaven National Laboratory, Center for Functional Nanomaterials, Upton, New York 11973, USA*
[3]*National Laboratory of Solid State Microstructures and Department of Materials Science and Engineering, Nanjing University, Nanjing 210093, China*

(Received 19 December 2014; accepted 23 February 2015; published online 5 March 2015)

We report a new 2D electron gas (2DEG) system at the interface between a Mott insulator, $LaTiO_3$, and a band insulator, $KTaO_3$. For $LaTiO_3/KTaO_3$ interfaces, we observe metallic conduction from 2 K to 300 K. One serious technological limitation of $SrTiO_3$-based conducting oxide interfaces for electronics applications is the relatively low carrier mobility (0.5-10 cm^2/V s) of $SrTiO_3$ at room temperature. By using $KTaO_3$, we achieve mobilities in $LaTiO_3/KTaO_3$ interfaces as high as 21 cm^2/V s at room temperature, over a factor of 3 higher than observed in doped bulk $SrTiO_3$. By density functional theory, we attribute the higher mobility in $KTaO_3$ 2DEGs to the smaller effective mass for electrons in $KTaO_3$. © *2015 Author(s). All article content, except where otherwise noted, is licensed under a Creative Commons Attribution 3.0 Unported License.* [http://dx.doi.org/10.1063/1.4914310]

The dominant operation mode of current electronics devices relies on the control of conduction channels in conventional semiconductors, such as Si. The electronic properties of these channels, including electron carrier density and mobility, determine the performance of the devices. One promising and versatile approach to achieving high carrier densities is to use interfaces involving perovskite oxide ABO_3 heterostructures. So far, only $SrTiO_3$ (STO) has been engineered to serve as the host for high density 2D electron gases (2DEGs), as exemplified by the interfacial systems of $LaAlO_3/SrTiO_3$ (LAO/STO),[1–15] $LaTiO_3/SrTiO_3$ (LTO/STO),[10,16–20] and $GdTiO_3/SrTiO_3$ (GTO/STO).[21–23]

For STO-based heterostructures, the 2DEG is believed to form through electrostatic doping at the interface between the perovskites. LAO, the prototypical ABO_3 oxide for STO-based 2DEGs, possesses a structure where the AO planes have a formal charge of $+1$ and the BO_2 planes have a charge of -1 in the [001] direction. In contrast, STO in the [001] direction is composed of charge neutral SrO and TiO_2 planes. At interfaces having TiO_2 terminated STO, the positively charged interfacial AO planes act as a sheet of donors, donating 0.5 electrons per unit cell (uc) to the TiO_2 layers (under ideal conditions) as illustrated in Fig. 1(a).[2,3,11–13,15] In this class of heterostructure, emergent phenomena such as 2D conduction, superconductivity,[7,14,17] and ferromagnetism[4,14,22] are observed at the interfaces. The sheet carrier density in LAO/STO[6,8,12] can be as high as 2×10^{13} cm^{-2}, which is difficult to achieve in conventional semiconductors. The carrier mobility at LAO/STO also reaches 800-10,000 cm^2/V s at low temperatures.[1,5,6] For LTO or GTO on STO, the carrier concentrations reach ~3-4 $\times 10^{14}$ cm^{-2}, and the mobilities range from 50 to 4,000 cm^2/V s at low temperatures.[17–19,21] However, the room temperature mobility is only 0.5-10 cm^2/V s for all 2DEGs based on STO.[1,5,6,18,19,21]

Motivated by the need for higher mobility systems, we investigate an alternate host for high carrier density 2DEGs,[24,25] $KTaO_3$ (KTO). In the case of LTO/KTO heterostructures, a polar discontinuity exists at the interface and thus should lead to the formation of a 2DEG, in direct analogy to STO-based 2DEGs. The discontinuity at LTO/KTO, however, is different from the STO-based 2DEGs in that KTO also has charged planes along (001): the AO planes are charged -1, and the BO_2 planes

 ©Author(s) 2015

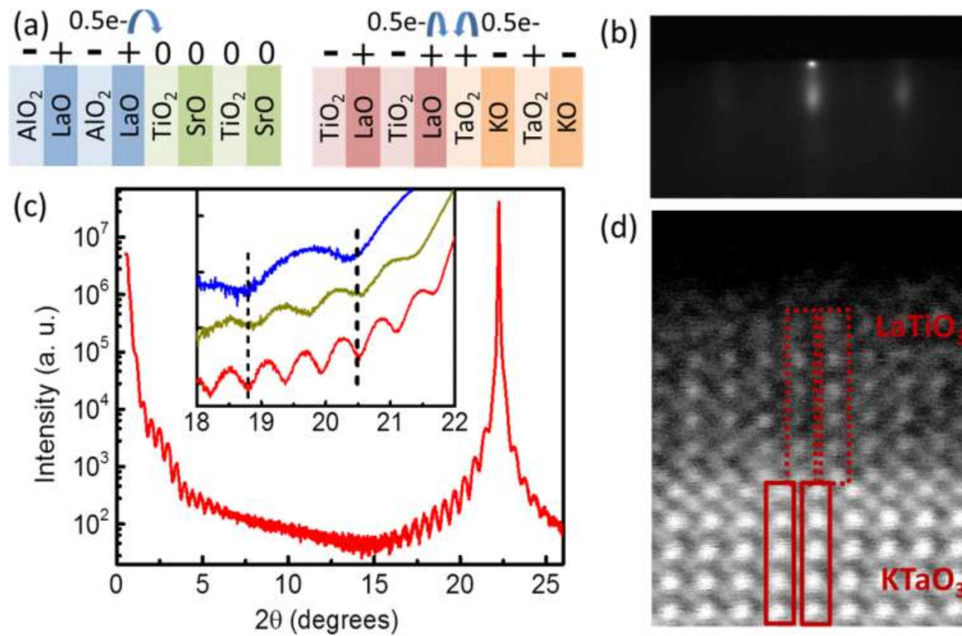

FIG. 1. (a) Schematic diagrams of the polar discontinuity and charge transfer of $LaAlO_3/SrTiO_3$ and $LaTiO_3/KTaO_3$. (b) Reflection high energy electron diffraction pattern of 12 uc $LaTiO_3/KTaO_3$. (c) X-ray diffraction pattern of 36 uc $LaTiO_3/KTaO_3$. The inset shows the finite thickness oscillations of 12 (blue), 24 (yellow), and 36 (red) uc $LaTiO_3/KTaO_3$. (d) Scanning transmission electron microscopy image showing the crystal structure of a 6 uc $LaTiO_3/KTaO_3$ heterostructure. The red boxes are a guide to the eye and highlight the heavier atoms (La (dashed line) and Ta (solid line)). From the relative locations of Ta and La at the interface, we find that the interface is TaO_2 terminated, as shown in panel (a).

are charged +1. These charges are opposite in sequence to those in LTO, where one has $(LaO)^{+1}$ and $(TiO_2)^{-1}$ planes. Therefore, at TaO_2-terminated LTO/KTO interfaces, the polar discontinuity has the same sign but twice the magnitude of STO-based heterostructures (see Fig. 1(a)).[26] The positively charged interfacial LaO and TaO_2 planes each donates 0.5 electrons to the interfacial TaO_2 layer. To the lowest order, the mobile electrons will reside primarily in the interfacial TaO_2 planes, where the Ta 5d orbitals forming the conduction band of KTO will determine the carrier properties.

Carriers in the Ta 5d orbitals of KTO should have a larger conductivity at room temperature. In the Drude model, the carrier mobility μ depends on the scattering time τ and effective mass m^* as $\mu = e\tau/m^*$, where e is the electronic charge. The conduction bands in STO heterostructures have primarily Ti 3d character, while the conduction bands in KTO have primarily Ta 5d character. Comparisons of the effective mass for electrons in bulk STO and KTO show that m^*/m_e is 0.49 for STO and 0.30 for KTO[24] (where m_e is the free-space electron mass). A second determining factor for mobility, the scattering rate, can be estimated by assuming that the carrier lifetime is dominated by electron-phonon scattering.[27] We note that the three lowest longitudinal optical phonon modes of STO have wavenumbers of 807, 473, and 173 cm^{-1}, similar to those of KTO, which are at 833, 423, and 188 cm^{-1}.[28] From this comparison, we expect similar scattering rates due to electron-phonon coupling for STO and KTO, and consequently a higher mobility for electron doped KTO due to the smaller effective mass of its carriers. To test these predictions, we grow LTO films of different thicknesses on KTO substrates. We achieve metallic conduction in high-density 2DEGs that do not involve STO.

Single-crystal (001) KTO (MTI crystal) wafers with dimensions $5 \times 5 \times 0.5$ mm^3 are used as the growth substrates, which appear colorless and transparent. The LTO thin films are grown in an oxide molecular beam epitaxy (MBE) system with a base pressure of ~1×10^{-10} Torr. Metal sources of La and Ti are thermally evaporated from effusion cells to react with molecular oxygen on the surface of the growing film. Metal fluxes are calibrated using a quartz crystal monitor with a growth rate of ~0.5 uc/min. It has been shown that oxygen vacancies are generated in KTO when T > 1000 °C, and the crystal becomes pale blue in color.[29] In order to preserve the stoichiometry of KTO,[30] the substrate

temperature is set at 750 °C during the growth, with no color change observed after growth. To protect LTO films from reacting with oxygen in air, a 6 nm-thick amorphous oxide TiO_x layer is deposited.

For the first 4 uc of film growth, reflection high energy electron diffraction (RHEED) indicates that the film is not fully crystallized (Fig. S1 of Ref. 31). At 12 uc, the LTO is observed by RHEED to be smooth and well ordered (Fig. 1(b)). After growth, the observation of clear finite-thickness fringes in X-ray diffraction (XRD) with a spacing that corresponds to the total film thickness shows that the initially disordered LTO fully recrystallizes. The measured spacing between the finite thickness oscillations confirms the film thicknesses to be 12, 24, and 36 uc-thick, corresponding to the as-deposited thicknesses (Fig. 1(c)).

We also use XRD to determine the lattice structure of LTO films. The bulk pseudo-cubic lattice parameter of LTO is ~3.97 Å, which is closely matched to the cubic lattice constant of KTO (3.98 Å). As a result, in the XRD pattern of 36 uc LTO/KTO (Fig. 1(c)), the (001) peaks of the substrate KTO and LTO film overlap.

Scanning transmission electron microscopy (STEM) images of the interfaces (Fig. 1(d)) show that the KTO wafers are terminated by TaO_2 planes, which is critical for achieving the polar discontinuity described in Fig. 1(a) and for accumulating interfacial electrons. The LTO films are epitaxial on the KTO substrates and demonstrate a fully crystalline interface. Ideally, one would like to control the termination to be KO or TaO_2 and study the polar discontinuity at the interfaces. However, to date, obtaining a KO terminated surface has proven difficult in experiments.

Devices are fabricated from thin films on KTO, with the LTO film thickness ranging from 3 uc to 24 uc. Transport measurements are made in the van der Pauw geometry, with contact to the 2DEG made using indium soldering at each corner of the square substrate. Each indium contact has an area of $\sim 300 \times 300\ \mu m^2$ for a $5 \times 5\ mm^2$ sample. Longitudinal and transverse resistivities are measured in a quantum design physical properties measurement system by four-point geometry, using a DC $<10\ \mu A$ to avoid Joule heating.

Figure 2(a) shows the 2D sheet resistance vs. temperature for 4, 6, and 12 uc-thick LTO/KTO. A metallic temperature dependence is observed for all thicknesses. In order to determine whether the metallicity in LTO/KTO originates in the bulk of the films or at their interfaces, we plot the thickness dependence of the sheet resistance at three different temperatures in Fig. 2(b). There is no monotonic decrease in resistivity with thickness, as would be expected for conduction through bulk LTO. The thickness dependence in Fig. 2(b) strongly suggests that the conduction in LTO/KTO heterostructures is confined to the interface, consistent with the formation of a 2DEG in the KTO.

Measurements of carrier density also provide important information on the conduction mechanism. To determine the carrier densities, Hall measurements of the transverse resistance $R_{XY}(B)$ are made as a function of temperature and field. $R_{XY}(B)$ is found to depend linearly on B up to $B = 5$ T in all samples (Fig. S2 of Ref. 31), representing single-channel conduction. From the slope

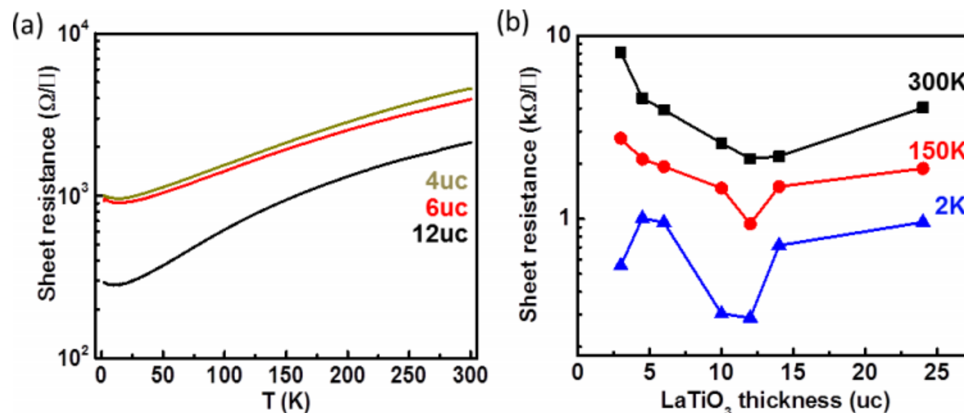

FIG. 2. (a) Metallic temperature dependence of the sheet resistance is observed in 4 uc (yellow), 6 uc (red), and 12 uc (black) $LaTiO_3/KTaO_3$. (b) Sheet resistance at T = 300 K (black), 150 K (red), and 2 K (blue) shows no monotonic dependence on $LaTiO_3$ thickness.

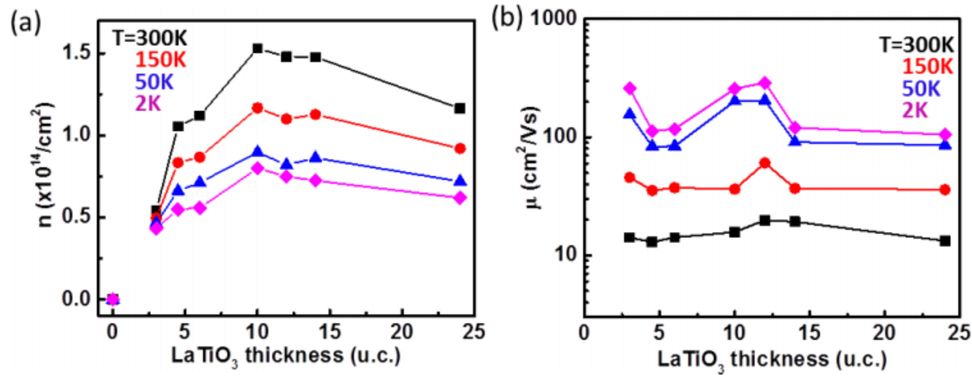

FIG. 3. Thickness dependence of (a) n and (b) μ of $LaTiO_3/KTaO_3$ at 300 K (black), 150 K (red), 50 K (blue), and 2 K (magenta). The lines connecting the data are a guide to the eye.

of $R_{XY}(B)$, we determine that the carriers in LTO/KTO are electrons, with a sheet density on the order of 1×10^{14} cm^{-2} (Fig. 3(a)), the sign of which is consistent with the observed TaO_2 termination and expected doping due to a polar discontinuity. From the measured carrier density and resistance, we derive the Hall mobility μ and plot its thickness dependence in Fig. 3(b).

We now turn to the first principles theory to elucidate certain microscopic aspects of the interface. Density functional theory (DFT) has been successful in predicting key elements of the electronic structure of interfaces at polar interfaces.[3,11,13,15] To theoretically study the metallicity and higher mobility in LTO/KTO, DFT is used to predict the electronic structure of LTO/KTO heterostructures with TaO_2-terminated KTO. The details of the methodology are described in Ref. 31. In brief, we use plane waves and pseudopotentials[32] together with the LSDA + U correction[33] for Ti 3d states.

The first system studied theoretically is a 4.5 uc LTO/4.5 uc KTO superlattice where all interfaces are LaO/TaO_2. This type of non-stoichiometric superlattice follows previous theoretical studies of polar interfaces such as LAO/STO.[13] Such a non-stoichiometric system enforces the addition, i.e., doping, of one electron per LaO/TaO_2 interface (per 1×1 interfacial unit cell) and describes the distribution electrons in the interfacial region regardless of their origin. For a polar mechanism, it models the thick LTO limit where the polar charge transfer to the interface is complete.

As discussed above, the polarity in both materials enforces electron accumulation at the interface. Given that Ta^{5+} is fully ionized with a large +5 formal charge while Ti^{3+} has one valence electron, we expect the interfacial electrons to prefer the lower energy Ta sites. The calculations confirm this: Figure 4 shows that the Fermi level crosses bands that have primarily Ta 5d character, while bands with Ti 3d character are either above or below the Fermi level. Specifically, LTO is an AFM insulator with full spin-polarization on each Ti site: one electron from each Ti^{3+} site fills a single, narrow, spin-polarized energy band that is separated from the unoccupied bands by an energy gap. Both types of LTO bands are visible in Fig. 4(a). The LTO is in a bulk-like, insulating configuration. Figure 4(b) shows that the interfacial electrons inhabit partially filled Ta 5d bands that cross the Fermi level and create interfacial conductivity. We calculate an electron effective mass m^*/m_e of 0.34 for the lowest energy interfacial Ta 5d-dominated bands which should be compared to 0.49 for 2DEGs in STO.[24] For reference, the Ti 3d dominated bands in Fig. 4(b) LTO have $m^*/m_e = 1.1$.

The second system studied theoretically uses stoichiometric LTO films on KTO substrates in order to explicitly demonstrate the polar mechanism for formation of the interfacial electron gas. As detailed in the supplementary material (see Fig. S3 of Ref. 31), we see the expected behavior where electrons are transferred from the surface region of the LTO film to the interfacial KTO regions and form the interfacial conducting channel.

The theory predicts a charge transfer and resulting metallicity at the interface, but there are other possible reasons for conduction we observe in the experiment. To rule out conduction from the bulk KTO substrate and the capping layer, we fabricate control samples with only KTO and the TiO_x protective overlayers, which undergo the same thermal cycling as during growth of LTO. The control

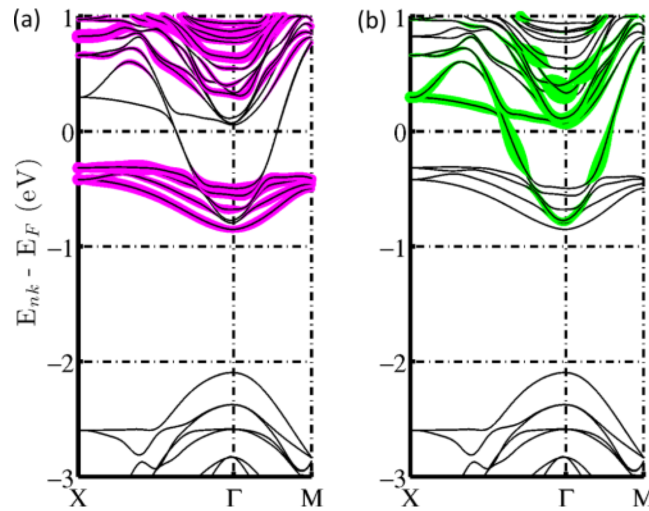

FIG. 4. *Ab initio* DFT band structure of $LaTiO_3/KTaO_3$ heterostructures with AFM order. Black curves indicate the electronic bands. Every band wave function is projected onto Ti 3d (magenta in panel (a)) and Ta 5d (green in panel (b)) atomic orbitals: larger projections correspond to thicker coloring. The Fermi level is at zero energy and crosses dispersive bands of Ta 5d character which have small effective mass. The interfacial conducting bands contain 1 electron per 1 × 1 interfacial unit cell.

samples are highly resistive, with a room temperature resistance of 5 MΩ, 3-4 orders of magnitude higher than the resistance of LTO/KTO heterostructures.

To explore possible conduction caused by the doping of La atoms in the KTO due to diffusion during growth, we have fabricated a control sample of 12 uc of LaO_x on KTO, which is expected to have the same level of La diffusion as the LTO/KTO samples. These structures exhibit an insulating temperature dependence, with a resistance of ~400 kΩ at T = 20 K and 21 kΩ at T = 300 K, at least one order of magnitude higher than the 12 uc LTO/KTO sample. The carrier density of the LaO_x sample is also about one order of magnitude lower at all temperatures. The diffusion of La atoms into KTO does not explain our transport results.

Bulk LTO films grown on STO are reported to conduct in Ref. 19, which may be due to ~2% compressive strain. LTO films grown with less strain on $GdScO_3$,[19] $DyScO_3$,[19] and Si[20] remain insulating. The lattice mismatch for LTO/KTO heterostructures is <0.5% and similar to the value for LTO/$GaScO_3$, which is insulating. We expect no bulk LTO conduction, and, indeed we do not observe a monotonic thickness dependence in resistivity (Fig. 2). Therefore, we rule out conduction in bulk LTO and KTO, the capping layer, or at interfaces created by intermixing La atoms.

While the origin of the conduction at the LTO/KTO interface is the same as that for LTO/STO, we expect that some of the details of the transport behavior for LTO/KTO interfaces will be different from that of LTO/STO. For example, non-linear Hall measurements have been observed for LTO/STO at low temperatures and attributed to two-carrier conduction.[18,34] We observe a single type of carrier in Hall measurements for LTO/KTO interfaces, consistent with a single band crossing the Fermi level (Fig. 4).

The magnitude of the maximum carrier concentration is lower than one expects from the polar discontinuity mechanism. A smaller than expected carrier concentration is also observed for the LAO/STO 2DEG,[6,8,12] with two mechanisms having been proposed to explain this observation. First, defects[11] induced by interfacial mixing may result in some of the carriers becoming immobile, so that only ~10% of the carriers are mobile and measured in electrical transport. The second mechanism, proposed in Ref. 15, asserts that carriers leave the interface to populate low energy and immobile surface trap states. We surmise that similar carrier reduction mechanisms may exist in LTO/KTO heterostructures.

At low temperatures, the mobility of LTO/KTO reaches ~300 cm^2/V s, consistent with the mobility for 2DEGs in LTO/STO and GTO/STO interfaces,[16–19] and one order of magnitude lower than in LAO/STO.[1,5,6] For many 2DEG systems, electron scattering with charged impurities is the

dominant scattering mechanism at low temperatures. It is likely that the STO and KTO wafers used in different experiments have different impurity levels. Charged impurities are also screened differently in STO and KTO due to their different dielectric constants. The dielectric constant of STO can be as high as 1.8×10^4 at low temperatures,[35] while the value for KTO is ~4000.[29] The smaller dielectric constant of KTO may lead to the lower mobility of LTO/KTO at low temperatures. However, at room temperature, the mobility of LTO/KTO reaches 21 cm^2/V s, higher than the reported values of 0.5-10 cm^2/V s in STO-based heterostructures. The dominant scattering mechanism at room temperature is electron-phonon scattering for the 2DEG hosting oxides, KTO and STO. Because KTO has optical phonon modes with similar energies compared to STO,[28] one can assume a similar electron-phonon scattering rate. We, therefore, expect that the smaller effective mass for KTO will lead to an enhancement of mobility of about 1.5 times that of STO system, in qualitative agreement with the mobility improvement we observe.

In conclusion, we have successfully induced a 2DEG at $LaTiO_3/KTaO_3$ interfaces. Metallic transport is observed in 3–24 uc heterostructures, where the carrier density increases with thickness to $1.5 \times 10^{14}/cm^2$ at 12 uc. Compared to $SrTiO_3$, the polarity of $KTaO_3$ translates into twice as high as an electron accumulation at polar-polar interfaces involving $KTaO_3$. First principles predictions of the 2DEG show that a smaller effective carrier mass is achieved in Ta 5d bands compared to Ti 3d bands. The smaller effective mass leads to higher room temperature mobilities observed in the experiments. This work demonstrates a new route to achieve higher interfacial carrier densities and mobilities in perovskite heterostructures through the use of alternative oxides that host the 2DEGs.

This research is sponsored by the AFOSR under Grant No. FA9550-12-1-0279. S.I.B. acknowledges support from the National Science Foundation DMR 1119826 (CRISP). The work at the Center for Functional Nanomaterials, Brookhaven National Laboratory is supported by the U.S. Department of Energy, Office of Basic Energy Sciences Division of Materials Science and Engineering, under Contract No. DE-AC02-98CH10886. X.S. thanks the China Scholarship Council and Brookhaven National Laboratory for financial support.

[1] A. Ohtomo and H. Y. Hwang, Nature **427**(6973), 423 (2004).
[2] N. Nakagawa, H. Y. Hwang, and D. A. Muller, Nat. Mater. **5**(3), 204 (2006).
[3] R. Pentcheva and W. E. Pickett, Phys. Rev. B **74**(3), 035112 (2006); J. Lee and A. A. Demkov, Phys. Rev. B **78**(19), 193104 (2008); R. Pentcheva and W. E. Pickett, Phys. Rev. B **78**(20), 205106 (2008); H. H. Chen, A. M. Kolpak, and S. Ismail-Beigi, Phys. Rev. B **79**(16), 161402 (2009); R. Pentcheva and W. E. Pickett, Phys. Rev. Lett. **102**(10), 107602 (2009); W. Son, E. Cho, B. Lee, J. Lee, and S. Han, Phys. Rev. B **79**(24), 245411 (2009); H. H. Chen, A. M. Kolpak, and S. Ismail-Beigi, Adv. Mater. **22**(26-27), 2881 (2010).
[4] A. Brinkman, M. Huijben, M. Van Zalk, J. Huijben, U. Zeitler, J. C. Maan, W. G. Van der Wiel, G. Rijnders, D. H. A. Blank, and H. Hilgenkamp, Nat. Mater. **6**(7), 493 (2007).
[5] G. Herranz, M. Basletic, M. Bibes, C. Carretero, E. Tafra, E. Jacquet, K. Bouzehouane, C. Deranlot, A. Hamzic, J. M. Broto, A. Barthelemy, and A. Fert, Phys. Rev. Lett. **98**(21), 216803 (2007).
[6] A. Kalabukhov, R. Gunnarsson, J. Borjesson, E. Olsson, T. Claeson, and D. Winkler, Phys. Rev. B **75**(12), 121404 (2007).
[7] N. Reyren, S. Thiel, A. D. Caviglia, L. F. Kourkoutis, G. Hammerl, C. Richter, C. W. Schneider, T. Kopp, A. S. Ruetschi, D. Jaccard, M. Gabay, D. A. Muller, J. M. Triscone, and J. Mannhart, Science **317**(5842), 1196 (2007).
[8] W. Siemons, G. Koster, H. Yamamoto, W. A. Harrison, G. Lucovsky, T. H. Geballe, D. H. A. Blank, and M. R. Beasley, Phys. Rev. Lett. **98**(19), 196802 (2007); M. Basletic, J. L. Maurice, C. Carretero, G. Herranz, O. Copie, M. Bibes, E. Jacquet, K. Bouzehouane, S. Fusil, and A. Barthelemy, Nat. Mater. **7**(8), 621 (2008).
[9] A. D. Caviglia, S. Gariglio, N. Reyren, D. Jaccard, T. Schneider, M. Gabay, S. Thiel, G. Hammerl, J. Mannhart, and J. M. Triscone, Nature **456**(7222), 624 (2008).
[10] C. Cen, S. Thiel, G. Hammerl, C. W. Schneider, K. E. Andersen, C. S. Hellberg, J. Mannhart, and J. Levy, Nat. Mater. **7**(4), 298 (2008).
[11] Z. S. Popovic, S. Satpathy, and R. M. Martin, Phys. Rev. Lett. **101**(25), 256801 (2008).
[12] Y. Segal, J. H. Ngai, J. W. Reiner, F. J. Walker, and C. H. Ahn, Phys. Rev. B **80**(24), 241107 (2009).
[13] H. H. Chen, A. M. Kolpak, and S. Ismail-Beigi, Phys. Rev. B **82**(8), 085430 (2010).
[14] J. A. Bert, B. Kalisky, C. Bell, M. Kim, Y. Hikita, H. Y. Hwang, and K. A. Moler, Nat. Phys. **7**(10), 767 (2011).
[15] A. Janotti, L. Bjaalie, L. Gordon, and C. G. Van de Walle, Phys. Rev. B **86**(24), 241108 (2012).
[16] H. Ishida and A. Liebsch, Phys. Rev. B **77**(11), 115350 (2008).
[17] J. Biscaras, N. Bergeal, A. Kushwaha, T. Wolf, A. Rastogi, R. C. Budhani, and J. Lesueur, Nat. Commun. **1**, 89 (2010).
[18] J. S. Kim, S. S. A. Seo, M. F. Chisholm, R. K. Kremer, H. U. Habermeier, B. Keimer, and H. N. Lee, Phys. Rev. B **82**(20), 201407 (2010).
[19] F. J. Wong, S. Baek, R. V. Chopdekar, V. V. Mehta, H. Jang, C. Eom, and Y. Suzuki, Phys. Rev. B **81**(16), 161101 (2010).
[20] E. N. Jin, L. Kornblum, D. P. Kumah, K. Zou, C. C. Broadbridge, J. H. Nhai, C. H. Ahn, and F. J. Walker, APL Mater. **2**, 116109 (2014).
[21] P. Moetakef, T. A. Cain, D. G. Ouellette, J. Y. Zhang, D. O. Klenov, A. Janotti, C. G. Van de Walle, S. Rajan, S. J. Allen, and S. Stemmer, Appl. Phys. Lett. **99**(23), 232116 (2011).

[22] P. Moetakef, J. Y. Zhang, A. Kozhanov, B. Jalan, R. Seshadri, S. J. Allen, and S. Stemmer, Appl. Phys. Lett. **98**(11), 112110 (2011).
[23] P. Moetakef, J. R. Williams, D. G. Ouellette, A. P. Kajdos, D. Goldhaber-Gordon, S. J. Allen, and S. Stemmer, Phys. Rev. X **2**(2), 021014 (2012).
[24] V. R. Cooper, Phys. Rev. B **85**(23), 235109 (2012).
[25] K. Ueno, S. Nakamura, H. Shimotani, H. T. Yuan, N. Kimura, T. Nojima, H. Aoki, Y. Iwasa, and M. Kawasaki, Nat. Nanotechnol. **6**(7), 408 (2011).
[26] J. Thompson, J. Hwang, J. Nichols, J. G. Connell, S. Stemmer, and S. S. A. Seo, Appl. Phys. Lett. **105**(10), (2014).
[27] A. Verma, A. P. Kajdos, T. A. Cain, S. Stemmer, and D. Jena, Phys. Rev. Lett. **112**(21), 216601 (2014).
[28] A. S. Barker, Phys. Rev. **145**(2), 391 (1966).
[29] S. H. Wemple, Phys. Rev. **137**(5A), 1575 (1965).
[30] H. M. Christen, L. A. Boatner, J. D. Budai, M. F. Chisholm, L. A. Gea, P. J. Marrero, and D. P. Norton, Appl. Phys. Lett. **68**(11), 1488 (1996).
[31] See supplementary material at http://dx.doi.org/10.1063/1.4914310 for the growth of $LaTiO_3$ at the interfaces, Hall measurements, methodological details of the *ab initio* calculations, and thin film *ab initio* results.
[32] P. Hohenberg and W. Kohn, Phys. Rev. **136**(3B), B864 (1964); W. Kohn and L. J. Sham, Phys. Rev. **140**(4A), A1133 (1965); J. P. Perdew and A. Zunger, Phys. Rev. B **23**(10), 5048 (1981); M. C. Payne, M. P. Teter, D. C. Allan, T. A. Arias, and J. D. Joannopoulos, Rev. Mod. Phys. **64**(4), 1045 (1992).
[33] V. I. Anisimov, F. Aryasetiawan, and A. I. Lichtenstein, J. Phys.: Condens. Matter **9**(4), 767 (1997).
[34] R. Ohtsuka, M. Matvejeff, K. Nishio, R. Takahashi, and M. Lippmaa, Appl. Phys. Lett. **96**(19), (2010).
[35] O. N. Tufte and P. W. Chapman, Phys. Rev. **155**(3), 796 (1967); R. Viana, P. Lunkenheimer, J. Hemberger, R. Bohmer, and A. Loidl, Phys. Rev. B **50**(1), 601 (1994).